Activated Blood Coagulation Factor X (FXa) Contributes to the Development of Traumatic PVR Through Promoting RPE Epithelial-Mesenchymal Transition

Han Han,[1] Xiao Zhao,[1] Mengyu Liao,[1] Yinting Song,[1] Caiyun You,[1] Xue Dong,[1,2] Xueli Yang,[1,3] Xiaohong Wang,[2] Bo Huang,[4] Mei Du,[2] and Hua Yan[1]

[1]Department of Ophthalmology, Tianjin Medical University General Hospital, Tianjin, China
[2]Laboratory of Molecular Ophthalmology, Department of Pharmacology and Tianjin Key Laboratory of Inflammation Biology, School of Basic Medical Sciences, Tianjin Medical University, Tianjin, China
[3]Department of Ophthalmology, The First Affiliated Hospital of Dali University, Yunnan, China
[4]Department of Ophthalmology, University of Mississippi Medical Center, Jackson, Mississippi, United States

Correspondence: Hua Yan, Tianjin Medical University General Hospital, No. 154, Anshan Road, Tianjin 300052, China; zyyyanhua@tmu.edu.cn.
Mei Du, Tianjin Medical University, No. 22, Qixiangtai Road, Tianjin 300070, China; dumei@tmu.edu.cn

HH and XZ contributed equally to the work presented here and should therefore be regarded as equivalent authors.

Received: October 24, 2020
Accepted: June 24, 2021
Published: July 20, 2021

Citation: Han H, Zhao X, Liao M, et al. Activated blood coagulation factor X (FXa) contributes to the development of traumatic PVR through promoting RPE epithelial-mesenchymal transition. *Invest Ophthalmol Vis Sci.* 2021;62(9):29. https://doi.org/10.1167/iovs.62.9.29

Purpose. Uncontrolled coagulation reactions contribute to pathological fibroproliferation in several organs, and yet their role in proliferative vitreoretinopathy (PVR) remains to be elucidated. In this study, we evaluated the profibrotic effects of FXa in RPE cells and in a mouse model of PVR.

Methods. FXa levels in the eyes of traumatic PVR patients and rabbit models of mechanical ocular trauma was measured by ELISA and immunohistochemistry. FXa-induced RPE EMT was assessed by examining cell proliferation, migration, tight junction changes, and expression of fibrotic markers. For *in vivo* study, FXa was injected into dispase-injured eyes, then intraocular fibrosis was evaluated by histological analysis and Western blotting. The therapeutic effect of FXa inhibitor was also examined in PVR mouse models.

Results. Vitreous FXa were higher in patients with traumatic PVR compared to patients with macular hole. Moreover, expressions of FXa and PAR1 were found in the epiretinal membranes from traumatic PVR patients. Vitreous FXa were markedly increased after mechanical ocular trauma in rabbits. *In vitro*, FXa stimulated RPE EMT characterized as ZO-1 disruption, compromised cell polarity, and increased fibronectin expressions. Co-injection of FXa and dispase in mice induced more severely damaged retinal structures, and increased α-SMA expressions than FXa or dispase treatment alone. Oral FXa or thrombin inhibitors significantly blocked intraocular fibrosis in PVR mouse models. FXa promoted phospho-activation of p38 in ARPE19 cells, which was dependent on PAR1. Moreover, TGF-βR inhibitor also significantly alleviated FXa-induced intraocular fibrosis in mice.

Conclusions. FXa promotes intraocular fibrosis in mice via mechanisms involving RPE activation.

Keywords: proliferative vitreoretinopathy, activated coagulation factor X, retinal pigment epithelial, epithelial-mesenchymal transition

Proliferative vitreoretinopathy (PVR) is a vision-threatening complication of mechanical ocular trauma that occurs in 40% to 60% of patients with open-globe injury.[1] The key cellular events underling PVR development is the migration and proliferation of retinal cells following a retinal break, which further participate in epiretinal membrane (ERM) formation in the periretinal area, and vision loss occurs when ERM contracts and causes a tear of the retina. Current treatment options for PVR are vitreous surgery to remove fibrous tissue and to repair retinal detachment.[2–4] Despite recent improvements in surgical techniques, 58.9% patients with PVR have poor visual prognosis because of recurrent retinal detachment.[5] Therefore new strategies for prevention and treatment of PVR are urgently needed.

The precise mechanisms underlying ERM formation in PVR are not well understood, and retinal pigment epithelial (RPE) cells are the principal cell type found in ERM.[6] During retinal injuries, RPE monolayer is disrupted, and dislodged RPE cells are released into the vitreous cavity or subretinal space where they undergo epithelial-to-mesenchymal transition (EMT) into myofibroblast-like cells.[7,8] RPE EMT can be initialed by exposure of RPE cells to several cytokines and growth factors, for example, TGF-β plays a remarkable role in inducing the mesenchymal transition of RPE cells.[9,10] Besides, activation of coagulation factors occurs in retinal injures, in addition to their role in blood coagulation, they also possess an pro-inflammatory and pro-fibrotic effect.[11,12]

Activated factor X (FXa) is a key proteinase of the coagulation cascade that lie upstream of thrombin generation.[13]

Recent studies showed a critical role of FXa in pathological fibrosis in different organs systems including the lung, liver and kidneys.[13–15] The profibrotic activity of coagulation proteinases like FXa and thrombin was mediated through activation of the protease-activated receptor (PAR) 1–4, which thrombin mainly acts on PAR 1, 3, and 4, and FXa activates either PAR 1 or 2.[14] Previous studies reported mRNA expression of PAR1 and PAR3 in RPE cells, and FXa and thrombin exerted proinflammatory and profibrotic effect in cultured RPE cells mainly through PAR1.[11] Moreover, increased thrombin activity was observed in the vitreous of patients with rhegmatogenous retinal detachment (RRD) or PVR,[16] and such vitreous samples could stimulate the proinflammatory and profibrotic responses in ARPE-19 cells, suggesting a role of coagulation factors in PVR. As mentioned earlier, FXa occupies a central position of the intrinsic and extrinsic coagulation pathways that catalyzes the conversion of prothrombin to thrombin. Therefore, inhibition of coagulation with FXa inhibitor may offer additional efficacy for antifibrotic treatment by blocking the subsequent amplification cascade of thrombin production. Indeed, previous studies reported that FXa inhibition had a stronger effect than thrombin inhibition in reducing the rate of hepatic fibrosis in mouse,[17] suggesting that earlier inhibition of coagulation cascade as a promising therapeutic target for fibrotic disease.

To date, no study has investigated the *in vivo* effects of FXa on the development of PVR, and the clinical relevance of FXa in ERM formation after ocular trauma is unknown. In this study, we examined the expression of FXa in the eyes of human patients with traumatic PVR and in rabbits eyes after mechanical ocular trauma. We identified the effect and the mechanisms of FXa on RPE EMT in ARPE-19 cells. By injection of FXa with dispase, an agent known to induce PVR-like conditions in mice,[18] we further examined the profibrotic effect of FXa *in vivo* and investigated therapeutic potential of FXa signaling inhibition.

Materials and Methods

Collection of PVR Membranes and Vitreous

Human PVR membranes and vitreous were obtained during vitreoretinal surgeries from patients with traumatic PVR at Tianjin Medical University General Hospital. All procedures were followed in accordance with institutional guidelines, and all patients have provided their written informed consent form. The membranes were fixed in 4% paraformaldehyde for 30 minutes, then dehydrate with 30% sucrose overnight at 4°C. After snap frozen and embedding in OCT compound, the membranes were sectioned at the thickness of 20 um and stored at −8°C until analysis. Vitreous samples contaminated with blood were excluded. Concentration of FXa and TGF-β were measured with human FXa ELISA kits (ml026291; mlbio, Shanghai, China) and TGF-β ELISA kits (D710586, AMEKO, Shanghai, China), respectively.

Rabbit Models of Ocular Trauma

The rabbits were handled as the Association for Research in Vision and Ophthalmology animal statement and kept in the Experimental Animal Laboratory of Tianjin Orthopedic Institute. For making rabbit open-globe injury (OGI) model, a 5 mm parallel horizontal incision was made 6.0 mm behind the corneoscleral limbus, 0.5 hour later, the wound was sutured with aseptic technique. The rabbit closed-globe injury model was made using fluid percussion injury device (FPI), briefly, the hammer was set to an angle of 65°, then the center of the cornea in the right eye of the rabbit was hit once. After injury induction, approximately 0.1 ml of vitreous fluid was withdrawn for designated time point, and vitreous fluid was withdrawn only once for each rabbit. Concentrations of FXa were measured by an ELISA kit (DEIA-BJ2660; Creative Diagnostics, Shirley, NC, USA).

Mouse PVR Model

All the animals were approved by Tianjin Medical University Animal Ethics Committee, and adherence to Association for Research in Vision and Ophthalmology Animal Statement. Male C57Bl/6J mice received Oxybuprocaine Hydrochloride for local anesthesia and Tropicamide for iris dilatation, then were anesthetized with 10% chloral hydrate (3.5 µL/g). Intravitreal injections were performed under stereomicroscope, using a 10 µL Hamilton syringe and 33G needle. Control mice received 1 µL 2% BSA, while experimental mice received a single injection of dispase or FXa for designated dosage. Rivaroxaban (Bayer, Germany, 1 mg/g diet) and dabigatran (Boehringer Ingelheim, Germany, 10 mg/g diet) supplemented diet were given to the mouse for consecutive 14 days started immediately after dispase and FXa injection. For TGF-β inhibitor treatment, mice received daily intraperitoneal injection of 10 mg/kg LY2109761(HY12075; MedChemExpress, Monmouth Junction, NJ, USA) for consecutive 14 days started immediately after dispase and FXa treatment. Fourteen days later, fundus images and optical coherence tomography (OCT) were conducted using a Retinal Microscopic Imaging System (Phoenix Research Labs, Pleasanton, CA, USA). Eyes were enucleated for histologic analysis. The severity of PVR was graded based on a previous study,[19] and grading criteria are detailed in Supplementary Table S1.

Cell Culture

Human RPE cell line ARPE-19 cells were cultured in DMEM/F-12 medium containing 10% fetal bovine serum (both from Gibco, Thermo Fisher Scientific, Waltham, MA, USA) and 1% penicillin-streptomycin (Solarbio Life Science, Beijing, China) at 37°C and 5% CO_2, with culture media changed every other day. For *in vitro* studies, cells were starved in serum-free medium (SFM) overnight before indicated treatment.

Cell Viability

ARPE-19 cells were seeded on 96-well plates at a density of 1×10^4 cells per well. After exposed to FXa for 24 hours, cell viability was determined by Cell Counting Kit-8 assay (CCK-8; Dojindo Molecular Technologies, Inc., Kumamoto, Japan) according to the manufacturer's instructions. Briefly, 10 µL CCK8 solution was added to each well and incubated at 37°C for two hours, then absorbance was measured at 450 nm using a spectrophotometer (Thermo Fisher Scientific). Each experiment was performed in quintuplicate wells, and three independent experiments were undertaken.

Investigative Ophthalmology & Visual Science

Small Interfering RNA

The small interfering RNAs (siRNAs) of human PAR1 (GAACCCUGCUCGAAGGCUACUATT) for knockdown experiments were obtained from Genepharma (Shanghai, China). The experiments were performed according to the manufacturer's protocol. ARPE-19 cells were cultured to 70% confluence and then were transfected using 160 nM PAR1 siRNA. Cells were incubated with siRNA for 12 hours, then returned to normal culture medium. Experiments were performed at 48 hours after transfection.

Western Blot

ARPE-19 cells or mouse retinas were lysed in RIPA buffer for 30 minutes on ice. Then lysates were centrifuged at 12,000 rpm for 20 minutes at 4°C. Total protein concentration was quantified by BCA assay (Solarbio, Life Science). Equal amounts of protein were loaded and separated by sodium dodecyl sulfate–polyacrylamide gel electrophoresis (SDS-PAGE) and transferred to PVDF membranes. The membranes were incubated with primary antibodies overnight at 4°C, then were incubated with secondary antibodies for 1 h. Blots were detected with an automatic chemiluminescence analysis system (Millipore, Burlington, MA, USA). Quantification of blots was performed using ImageJ software.

Immunohistochemistry

ARPE-19 cells were seeded on coverslips in 12-well plates. After treatment, cells were fixed in 4% PFA for 15 minutes and blocked in 0.3% TritonX-100, 2% BSA in PBS for one hour. After wash, cells were incubated with primary antibody overnight in humid chamber at 4°C, followed by incubation with secondary antibodies for one hour. Coverslips were examined under confocal microscope (Zeiss LSM 510; Zeiss, Oberkochen, Germany).

Mouse eyes were collected and fixed in 4% PFA for one hour. Cornea and lens were removed, then RPE-choroid-sclera complex was peeled off from neural retina. RPE wholemounts were permeabilized with 1% Triton X-100/PBS and blocked with 5% goat serum at 4°C with rocking. Then wholemounts were incubated with primary antibodies for two days on a shaker at 4°C. After washing, RPE wholemounts were incubated with secondary antibodies and propidium iodide (PI, 1:100; Sigma-Aldrich Corp., St. Louis, MO, USA) for two hours. RPE wholemounts were examined under a confocal microscope.

Transwell Assay

ARPE-19 cells were seeded in the upper chamber of 24-well Transwell plates (Corning, Inc., Corning, NY, USA) in 100 µL DMEM/F12 media containing 0.5% FBS. The lower compartment was filled with 600 µL DMEM/F12 media containing 10% FBS. Cells were treated with FXa or TGF-β2 for eight hours, then cells on the upper surface of the filter were removed and the migrated cells on the lower surface of the filter were fixed with 4% PFA and stained with 0.1% crystal violet for 30 minutes. Images were taken under a fluorescent microscope (Olympus Corporation, Tokyo, Japan), and migrating cells were counted using Image J software. The number of migrated cells in five random fields (magnification ×10) of each chamber was counted.

Scratch Assay

To analyze cell migration, ARPE-19 cells were seeded on six-well plates at a density of 1×10^5 cells per well. A wound was made by scraping RPE monolayer with a 20 µL pipette tip, then cells were treated and images were taken under a light microscope (Olympus Corporation) at zero hour and 24 hours after scratch. The percentage of RPE migration was analyzed with Image J software. At least three fields (magnification × 10) of view per treatment of three independent experiments were quantified.

To analyze cell polarity, ARPE-19 cells were seeded on 12-well plates with glass coverslips. Cells were scratched and treated with different agents for 24 hours. Then cells were fixed in 4% PFA for 15 minutes and incubated with anti-GM130 overnight at 4°C, followed by incubation with FITC-conjugated secondary antibodies for one hour. After washing, coverslips were counterstained with DAPI and visualized under confocal microscope (Zeiss LSM 800; Zeiss).

BrdU Assay

ARPE-19 cells were seeded on 12-well plates with coverslips. After cells were treated, BrdU (10 µM, B5002; Sigma-Aldrich) was added and incubated for four hours at 37°C. Then cells were fixed in 4% PFA/PBS for 20 minutes and blocked in 2% BSA 0.3% Triton X-100/PBS for 30 minutes. Antigen unmasking was performed by adding ice-cold 0.1 M HCl for 20 minutes and then 2M HCl for 30 minutes, followed by neutralization with sodium borate buffer for 15 minutes. After washing, coverslips were incubated with anti-BrdU (ab6326; Abcam, Cambridge, MA, USA) overnight at 4°C, and incubated with secondary antibody for one hour. Coverslips were counterstained with DAPI and visualized under confocal microscope (Zeiss LSM 800; Zeiss). At least three fields (magnification ×40) of view per treatment of three independent experiments were quantified.

Statistical Analysis

All studies were presented as the mean ± SEM from at least three independent experiments. Data were analyzed using *t* test or one-way ANOVA. Significant differences were considered at $P < 0.05$. All statistical analyses were performed using Prism software (GraphPad, San Diego, CA, USA).

Results

Vitreous Levels of FXa Were Increased in Patients With Traumatic PVR and in Rabbit Eyes After Mechanical Ocular Trauma

To explore the involvement of FXa in traumatic PVR, we detected the expression of FXa in ERMs collected from PVR patients induced by trauma and nontrauma (RD patients complicated with PVR) by immunostaining. We found the expressions of FXa were co-localized with α-SMA positive cells (Supplementary Fig. S1), and expressions of FXa were more pronounced in the ERMs collected from PVR patients induced by trauma (TPVR) than non-trauma (Figs. 1A, 1B). To explore whether FXa localizes to RPE cells, we performed double staining for FXa and RPE65 as RPE-specific marker. We found the fluorescent signals of FXa were mostly co-localized with RPE65 in the ERMs from traumatic PVR patients (Figs. 1A, 1B). Furthermore, FXa levels were signif-

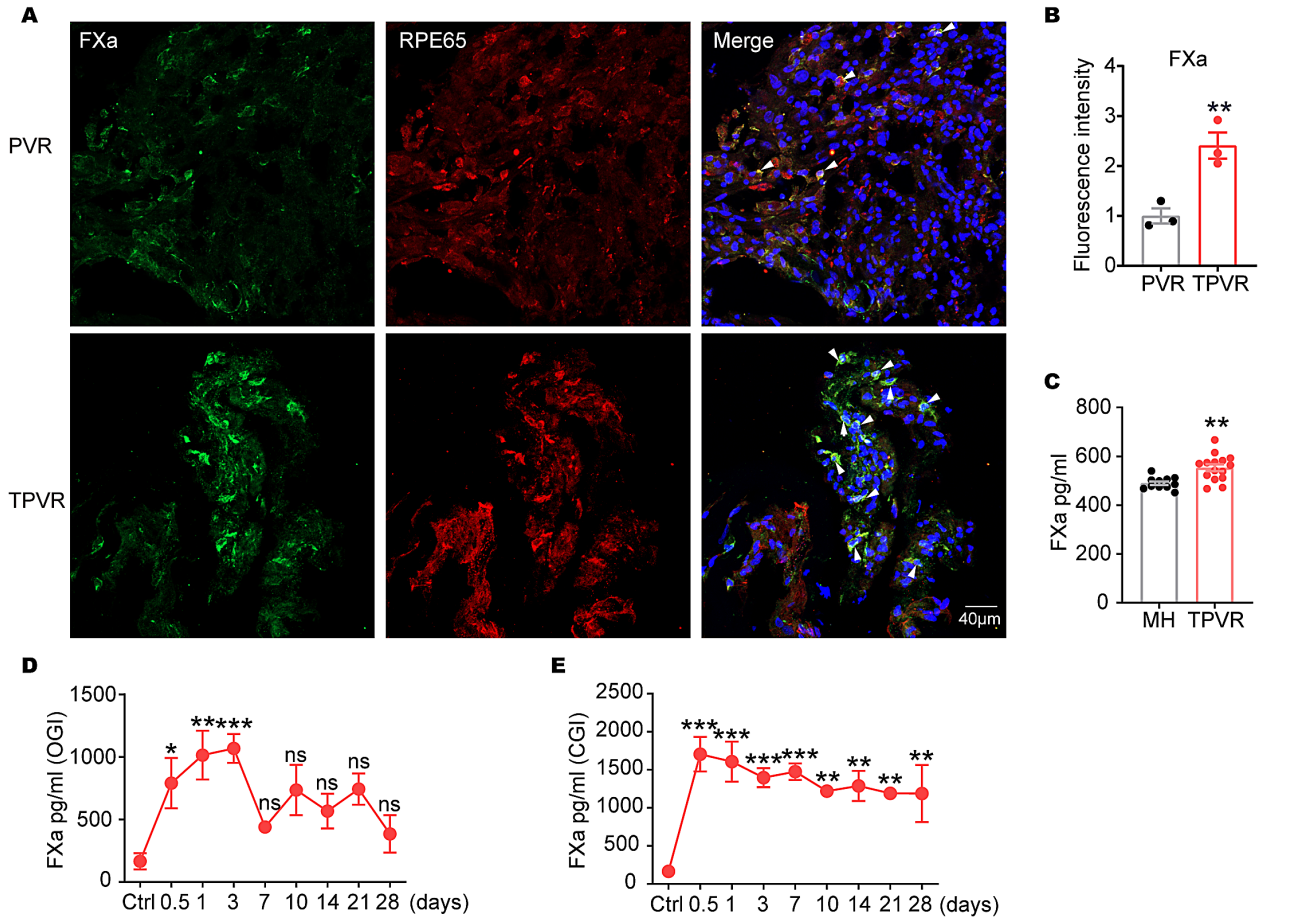

Figure 1. Ocular levels of FXa were significantly increased in patients with traumatic PVR and rabbit models of mechanical ocular trauma. (**A**) Representative confocal images of FXa and RPE65 immunostaining in epiretinal membrane isolated from TPVR patients and PVR patients. (**B**) Quantification of the FXa staining. (**C**) Vitreous levels of FXa were significantly higher in TPVR patients than macular hole (MH) patients. (**D**) ELISA measurement of vitreous FXa in rabbit models of open globe injury. (**E**) ELISA measurement of vitreous FXa in rabbit models of closed globe injury. n = 5 animals/time point. Data are presented as mean ± SEM, $^{*}P < 0.05$; $^{**}P < 0.01$; $^{***}P < 0.001$.

icantly increased in vitreous fluid samples from traumatic PVR patients compared to macular hole (MH) patients (Fig. 1C). To evaluate changes of FXa in the eye after ocular trauma, vitreous FXa were measured in rabbit eyes after open and closed globe injury. After OGI, vitreous FXa were significantly increased at 0.5 day and reached a peak at three days then declined steadily. The significance of vitreous FXa between OGI and control group was diminished at seven days after the injury (Fig. 1D). Similarly, after closed-globe injury, vitreous FXa were increased and reached a peak at 0.5 day, and then declined slightly, but the levels still remain high at 28 days after the injury (Fig. 1E). Altogether, these data showed increased vitreous levels of FXa in patients with traumatic PVR and in rabbit models of mechanical ocular trauma, and expressions of FXa in the ERMs from traumatic PVR patients, suggesting the involvement of FXa in PVR development after mechanical ocular trauma.

FXa Impairs RPE Cell Tight Junction and Cell Polarity, and Promotes RPE Cell Proliferation and Migration

After FXa treatment, RPE tight junctions, cell polarity, proliferation, and migration of RPE cells were analyzed. TGF-β2 was used as a positive control. We found FXa treatments resulted in disruption of ZO-1 in a dose dependent manner. Quantification of ZO-1 discontinuous rate showed that 25 nM FXa resulted in 25.94% loss of ZO-1 proteins in RPE cells, which is similar to the effect of 10 ng/mL TGF-β2 (31.83%) (Figs. 2A, 2B).

The loss of RPE polarity was another cellular change occurred during EMT.[20] To examine cell polarity change, we stained the GM130 (a Golgi marker protein) in ARPE-19 cells after scratch to assess the alignment of Golgi apparatus with the direction of cell migration. Typically, the directional migration of cells requires a polarized arrangement of the cytoskeleton, with microtubule tissue center and Golgi located at the leading edge of the cell.[21] Indeed, most of the untreated cells showed forward facing of Golgi at the leading edge of cell migration, in contrast, FXa-treated cells showed randomization in the direction of cell migration (Figs. 2C, 2D). Polarity Index was calculated as previously reported.[22] We found decreased polarity index in FXa 25 nM (11.75%) treated cells than untreated cells (45.67%), suggesting compromised RPE polarity upon FXa stimulation.

Next, we evaluated the effects of FXa on RPE cells proliferation and migration. In BrdU incorporation assay, we found marked increased BrdU+ cells in ARPE19 cells treated with FXa, and higher concentration of FXa (25 nM) showed even more BrdU+ cells (Figs. 2E, 2F). Similarly, CCK8 assay showed a dose-dependent increase of cell viability of RPE cells induced by FXa (Fig. 2G). Scratch assay showed that

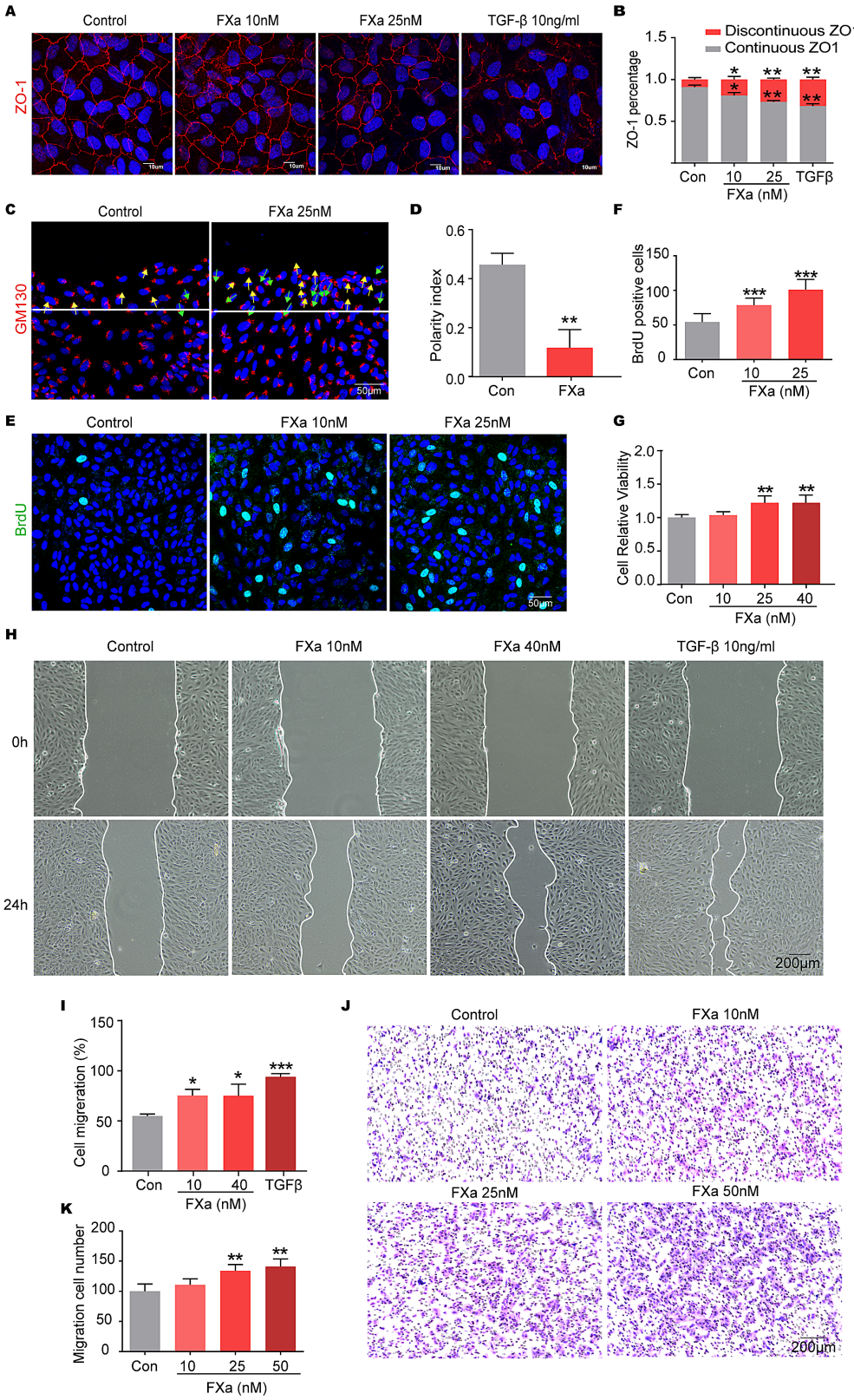

Figure 2. FXa impairs RPE tight junction and polarity and promotes cell proliferation and migration. ARPE-19 cells were treated with FXa or TGF-β2 as positive control for 24 hours, and the following experiments were performed: (**A**) Representative confocal fluorescent images of the tight junction protein ZO-1 in ARPE-19 cells. (**B**) Quantification of the discontinuous rate of ZO-1 staining. (**C**) ARPE-19 cells were scratched and fluorescent labeled with anti–GM130 to measure cell polarity. (**D**) Quantification of cell polarity index. (**E, F**). Measurement of RPE cell proliferation by BrdU assay. (**G**) Measurement of RPE cell viability by CCK8 assay. (**H**) Measurement of RPE cell migration after 24 hours of FXa or TGF-β treatment by Scratch assay. (**I**) Quantification of RPE cell migratory area in each group. (**J**) Transwell migration analysis of ARPE-19 cells treated with FXa for 8 h. (**K**) The number of migrated cells was quantified by examining images of six random fields from each group. Data are presented as mean ± SEM. *$P < 0.05$, **$P < 0.01$, ***$P < 0.001$.

Investigative Ophthalmology & Visual Science

24 hours after scratch, FXa resulted in increased migration of RPE cells toward the wound area (Figs. 2H, 2I). Likewise, in transwell system, migrating cells was significantly increased upon FXa stimulation, with 50 nM FXa showing the most potent effect (Figs. 2J, 2K).

FXa Promotes Matrix Deposition Both in RPE Cells and Mouse Model of PVR

To determine the effect of FXa on ECM deposition, expressions of the major matrix components fibronectin (FN) were analyzed. We found FN mRNA were significantly increased after 24 h of FXa treatment (Fig. 3A). The protein levels of FN were also markedly increased after FXa (25 nM) treatment at 24 h and even more at 48 h (Figs. 3B, 3C). Likewise, FN immunofluorescence confirmed increased expressions of FN in RPE cells in response to FXa stimulation (Figs. 3D, 3E).

To investigate the profibrotic effect of FXa *in vivo*, a dispase-induced PVR mouse model was used.[23] In this model, intravital injection of dispase induced a PVR-like condition characterized by retinal detachment and retinal folds, this exposed RPE cells to vitreous components which are known predisposing conditions associated with PVR development.[18] Fundus images and histological analysis revealed the presence of retinal detachment in both dispase- and dispase+FXa–treated eyes, with the latter showed more severely damaged retinal structure (Fig. 3F). In comparison, injection of FXa alone did not induce any observable changes in retinal structure (Fig. 3F). In agreement with these results, OCT images clearly showed formation of epithelial membrane in retinas treated with dispase or dispase+FXa (Fig. 3F). We then evaluated the severity of PVR according to a grading scheme reported previously[19] and found that eyes that received dispase+FXa showed more severe PVR compared to eyes only received dispase (Fig. 3G). The formation of ERM was further evaluated by Masson trichrome collagen staining, and positive Masson staining was evident in retinas treated with dispase+FXa and dispase but not FXa treatment alone (Supplementary Fig. S2). Furthermore, α-SMA expressions were more pronounced in the dispase+FXa group than dispase or FXa alone treated retinas (Fig. 3H-I). Altogether, these data suggest that co-administration of FXa with dispase significantly accelerated intraocular fibrosis in mouse.

To examine RPE activation, the epithelial integrity of RPE was evaluated. Although RPE pigmentation still remained intact in all the groups (Supplementary Fig. S3), we observed a marked disruption of ZO-1 proteins in RPE wholemount in dispase injured eyes, and co-administration with FXa severely aggravated ZO-1 breakdown (Figs. 3J, 3K). Meanwhile, α-SMA expressions were increased in RPE wholemount from dispase or dispase+FXa treated eyes, with dispase+FXa treated eyes showed the most prominent expression (Fig. 3J). These data suggest a direct effect of FXa on RPE activation, which are likely contributing to FXa induced intraocular fibrosis.

Oral FXa Inhibitor Mitigated FXa-induced Intraocular Fibrosis in Mouse Model of PVR

To continue investigate the actual role of FXa in PVR pathogenesis *in vivo*, we applied rivaroxaban, a direct inhibitor of FXa, into the mice after dispase or dispase+FXa injection for 14 days, then the effect of rivaroxaban on intraocular fibrosis was evaluated by histological analysis and Western blotting. As the effects of thrombin on promoting RPE inflammation and EMT have been well reported in cultured RPE cells,[11,24,25] we also included the thrombin inhibitor dabigatran in our study to compare the effects of the two inhibitors on PVR development. The plasma concentrations of both inhibitors were measured by liquid chromatography–mass spectrometry (LC-MS/MS) after 14 days of the inhibitors diet. We found mean plasma concentration of rivaroxaban was 56.96 ng/mL in rivaroxaban group, and dabigatran was 24.43 ng/mL in dabigatran group (Supplementary Table S2).

Histological analysis of retinal sections showed that treatment with rivaroxaban alleviated the retinal structural damage and retinal detachment in dispase and dispase+FXa mice (Fig. 4A). Grading of PVR severity based on HE staining also revealed less severe PVR in dispase and dispase+FXa mice treated with rivaroxaban compared to mice that did not receive the anticoagulant (Fig. 4B). Next, we measured the expression of fibrotic marker, α-SMA and found application of rivaroxaban dramatically reduced α-SMA protein expression in mice treated with dispase (Figs. 4C, 4D). For mice treated with dispase+FXa, rivaroxaban also significantly reduced α-SMA levels (Figs. 4C, 4D), although to a lesser extent compared to the effect of rivaroxaban in dispase mice group. Similar to the effect of rivaroxaban, treatment with dabigatran also alleviated the retinal structural damage and retinal detachment in dispase and dispase+FXa mice (Fig. 4E), resulting in less severe PVR in mice treated with dabigatran than those did not receive the anticoagulant (Fig. 4F). In addition, application of dabigatran also significantly reduced the expression of α-SMA in dispase mice group (Figs. 4G, 4H). However, dabigatran did not show significant effect on reducing α-SMA expressions in dispase+FXa mice group (Figs. 4G, 4H). In summary, these data support a beneficial role of oral FXa inhibitor in improving PVR in dispase mouse models, and future clinical studies are needed to validate our results.

FXa Induced RPE EMT Depends on PAR1 and P38 Signaling

To unravel the mechanisms by which FXa induces RPE EMT, we first examined whether PAR receptors were activated by FXa in RPE cells. Upon FXa stimulation, PAR1 mRNA was significantly increased, while PAR2 mRNA remained unchanged (Figs. 5A, 5B). Western blot showed robust expression of PAR1 protein in RPE cells, whereas PAR2 protein showed only a faint band (Fig. 5C). Moreover, FXa stimulation increased the levels of cleaved PAR1 which peaked at 10 mins, indicating activation of PAR1 by FXa (Figs. 5C, 5D). Besides, we found abundant expression of PAR1 in the ERMs collected from traumatic PVR patients, which colocalized with the fibrotic marker α-SMA (Fig. 5E), suggesting a role for PAR1 in ERM formation. Several studies have revealed a central role of p38-MAPK signaling in PVR pathogenesis.[26,27] We found that FXa treatment significantly induced phosphor-activation of P38 in ARPE-19 cells starting at 10 minutes after treatment (Figs. 5F, 5G). We also found the phosphorylation of P38 were significantly increased in both dispase and dispase+FXa treated mice, supporting the role of P38 signaling in our mouse PVR model. Moreover, treatment with FXa inhibitor rivaroxaban significantly blocked P38 phosphorylation induced by dispase or dispase+FXa in mice (Figs. 5H, 5I). In addition, pretreat-

Investigative Ophthalmology & Visual Science

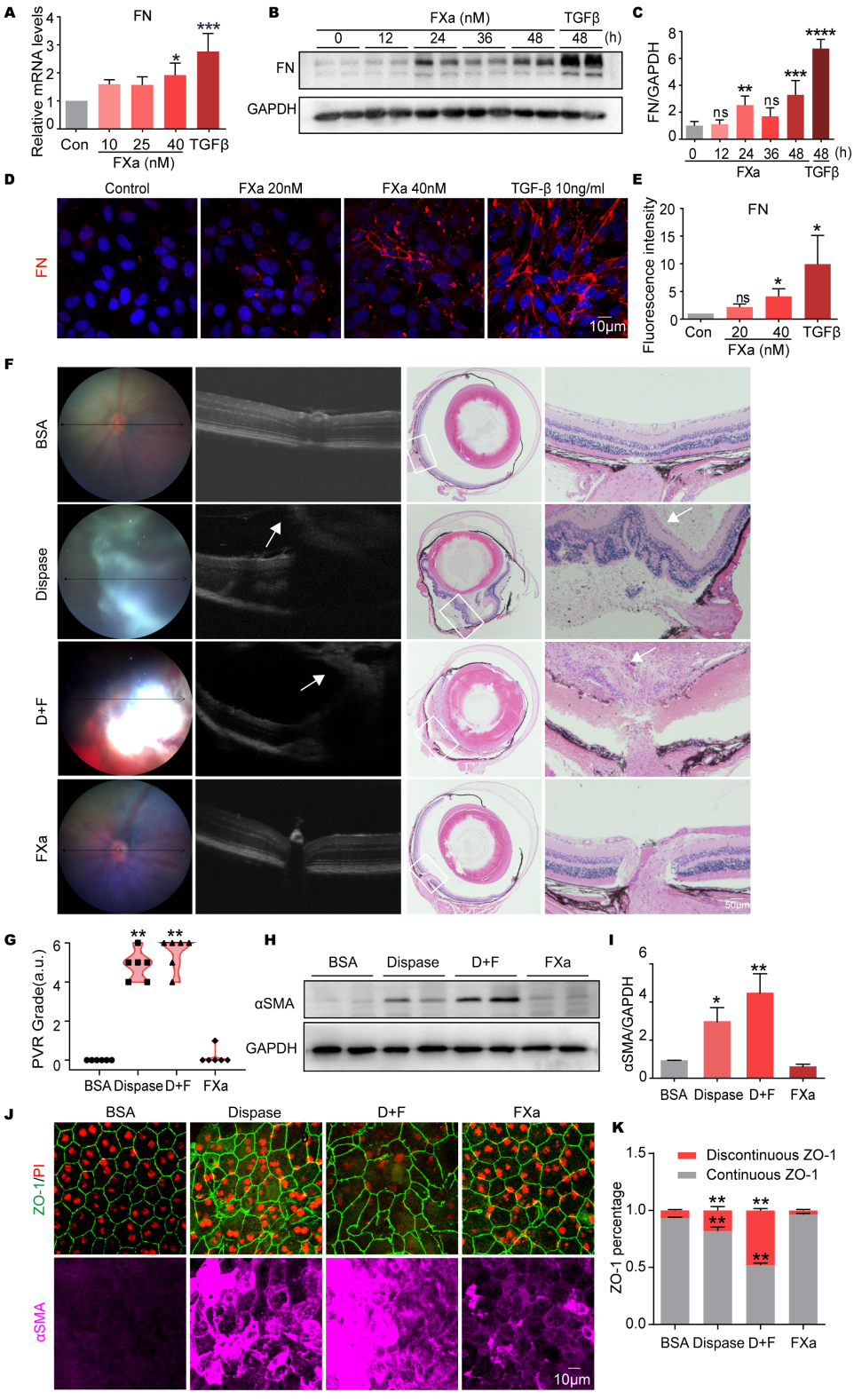

Figure 3. FXa promotes matrix deposition in RPE cells and in PVR mouse model. (**A**) Detection of FN mRNA expressions in ARPE-19 cells treated with FXa or TGF-β by qRT-PCR. FN, fibronectin. (**B**) Western blot measurement of FN levels in ARPE-19 cells treated with FXa (25 nM) or TGF-β2 10 ng/mL. (**C**) Relative FN expressions (normalized to GAPDH) were quantified. (**D**) Immunofluorescent labeling of FN in ARPE-19 cells treated with FXa or TGF-β2 for 24 hours. Nuclei were stained with DAPI. (**E**) Quantification of FN staining. (**F**) Representative OCT, retinal fundus images, and H&E histology of C57 mice aged 12 weeks that received intravitreal BSA, dispase (0.02U), FXa (40 nM) or dispase+FXa. The right panel shows higher magnification of the boxed area. D+F, Dispase+FXa. (**G**) Grading of PVR severity. (**H, I**). Western blot and densitometry analyses of α-SMA expression in retinas from C57 mice received intravitreal dispase (0.02 U) or Fxa (40 nM). The relative expression of α-SMA and was normalized to GAPDH. n $\geq$ 3 mice per treatment group. (**J**). Immunofluorescence staining of ZO-1 and α-SMA in RPE wholemount of C57 mice aged 12 weeks received dispase or FXa treatment. Images were taken from equatorial regions of retina. (**K**). Quantification of discontinuous rate of ZO-1 staining shown in **D**. Values are means $\pm$ SEM, $^{*}P < 0.05$, $^{**}P < 0.01$, $^{***}P < 0.001$.

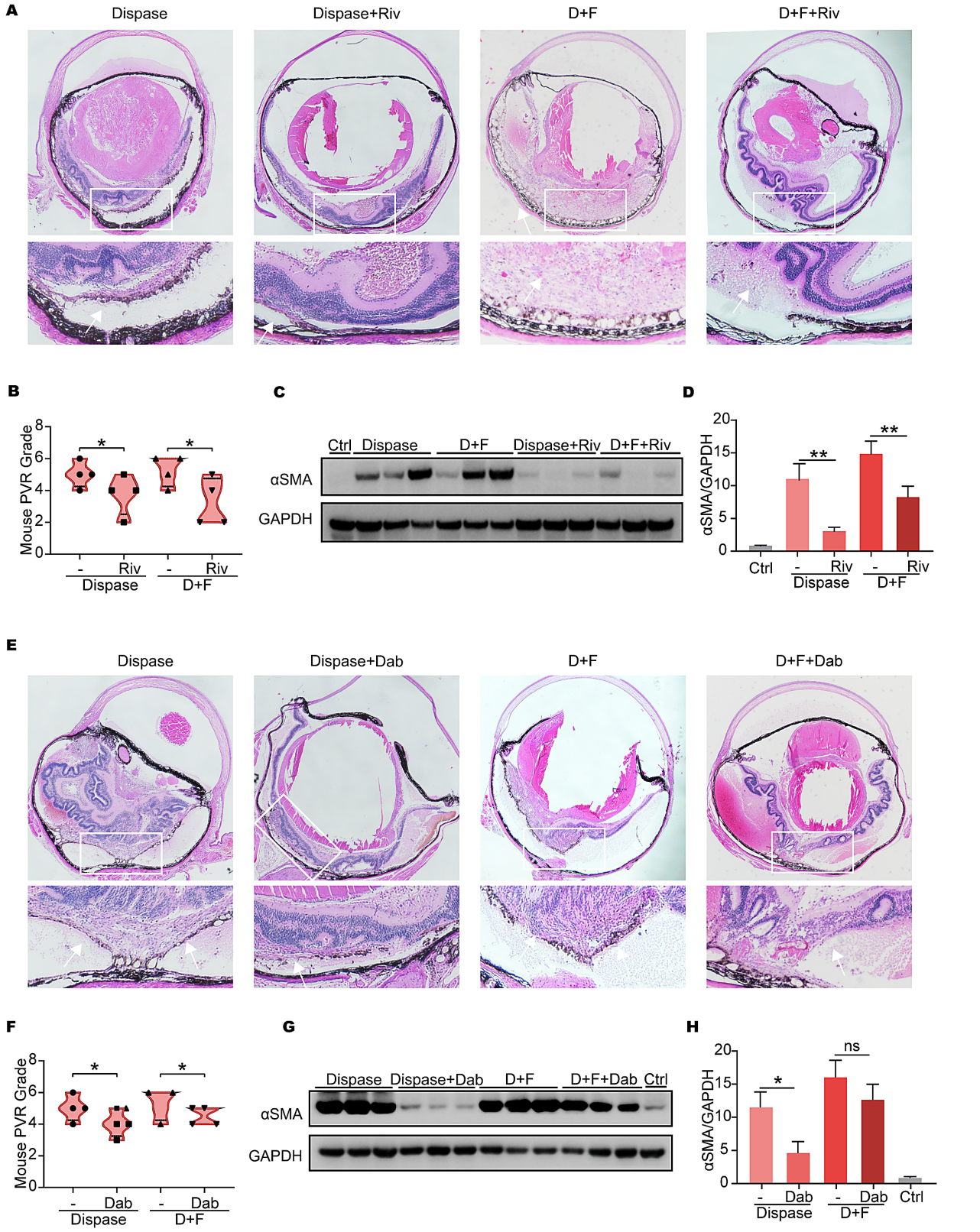

Figure 4. Oral FXa or thrombin inhibitor mitigated intraocular fibrosis in mouse model of PVR. (**A**) H&E stained retinal sections from dispase and dispase+FXa mice with or without pretreatment with rivaroxaban. Rab, Rivaroxaban; D+F, Dispase+FXa. (**B**) Grading of PVR severity based on **A**. (**C**). Western blot analysis of α-SMA in retinas of mice from designated treatment groups. (**D**) Quantification of the Western blot of α-SMA shown in **C**. The α-SMA protein expression was normalized to GAPDH. n ≥ 7 mice per treatment group. (**E**) H&E stained retinal sections from dispase and dispase+FXa mice with or without pretreatment with dabigatran. Dab, Dabigatran. (**F**) Grading of PVR severity based on **E**. (**G**) Western blot analysis of α-SMA expression in retinas of mice from designated treatment groups. (**H**). Quantification of the Western blot of α-SMA protein expression shown in **G**. The α-SMA protein expression was normalized to GAPDH. n ≥ 7 mice per treatment group. Values are means ± SEM, *$P < 0.05$, **$P < 0.01$.

Investigative Ophthalmology & Visual Science

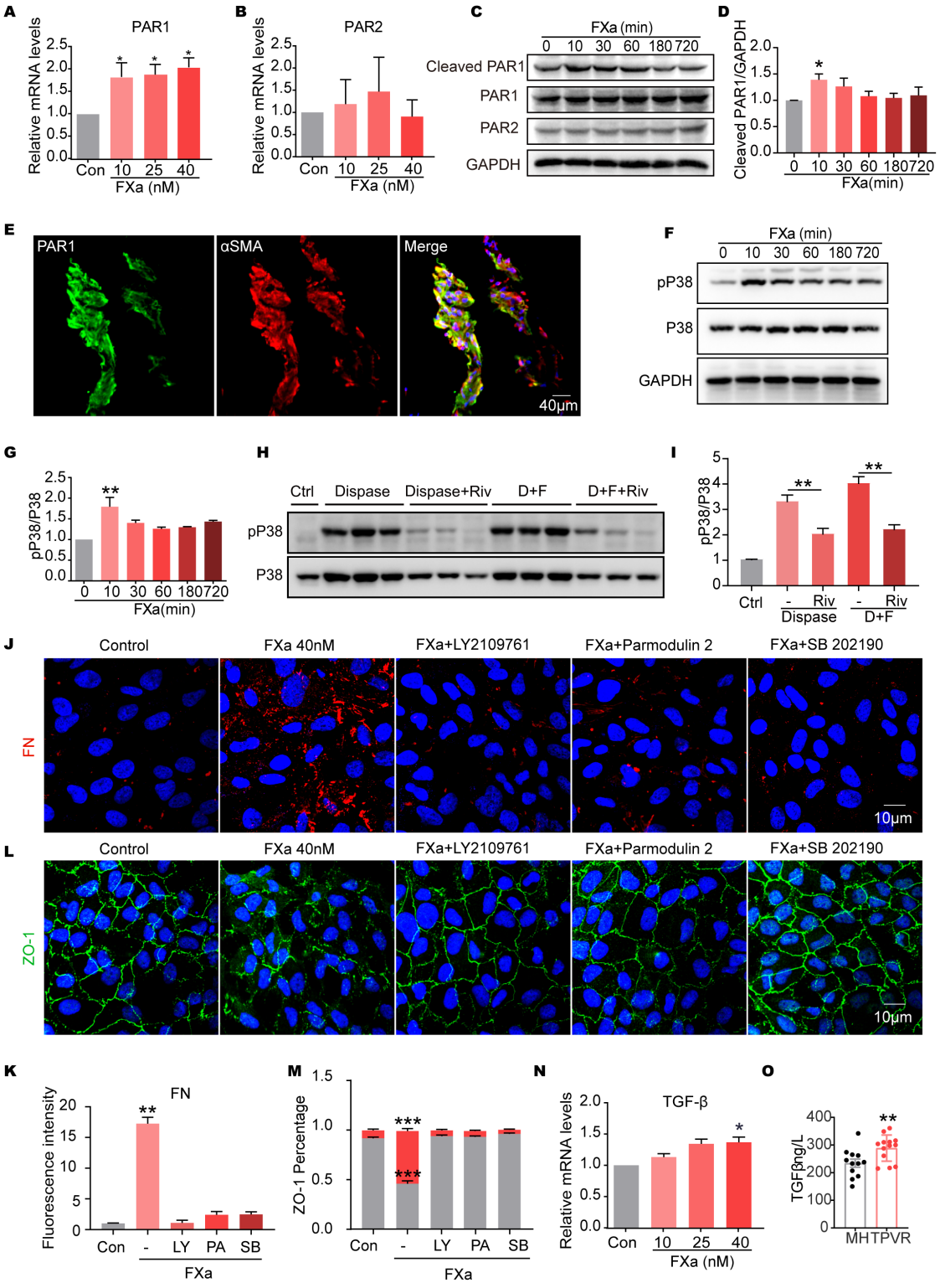

Figure 5. FXa induces RPE EMT through PAR1-P38 signaling and TGF-β signaling also played a role. (**A**, **B**) ARPE-19 cells were treated with FXa or TGF-β for 24 hours, then mRNA expression of PAR1 and PAR2 were detected by qRT-PCR. (**C**) ARPE-19 cells were treated with FXa (40 nM) for indicated time points, then expression of cleaved PAR1, PAR1 and PAR2 was analyzed by Western blot. (**D**) Quantification of the Western blot shown in **C**. (**E**) Representative confocal images of PAR1 and α-SMA immunostaining in the ERM from traumatic PVR patients. (**F**) ARPE-19 cells were treated with FXa (40 nM) for indicated time points, then expression of p- and total P38 was analyzed by immunoblotting. (**G**) Quantification of the Western blot shown in **F**. (**H**) Western blot of p- and total P38 in retinas of mice from designated treatment groups. (**I**) Quantification of the Western blot of pP38 shown in **H**. n $\geq$ 7 mice per treatment group. (**J**) FXa induced upregulation of fibronectin in ARPE-19 cells was downregulated by Parmodulin 2, LY2109761 or SB 202190 (P38 MAPK inhibitor). (**K**) Quantification of FN staining. LY, LY2109761; PA, Parmodulin 2; SB, SB 202190. (**L**) FXa-induced reduction of ZO-1 proteins were mitigated by pretreatment of Parmodulin 2, LY2109761 or SB 202190. (**M**) Quantification of discontinuous rate of ZO-1 staining. (**N**) ARPE-19 cells were treated with FXa or TGF-β for 24 hours, then mRNA expression of TGF-β were detected by qRT-PCR. (**O**) Measurement of vitreous levels of TGF-β in TPVR patients and MH patients. Values are means $\pm$ SEM, $^{*}P < 0.05$, $^{**}P < 0.01$, $^{***}P < 0.001$.

Investigative Ophthalmology & Visual Science

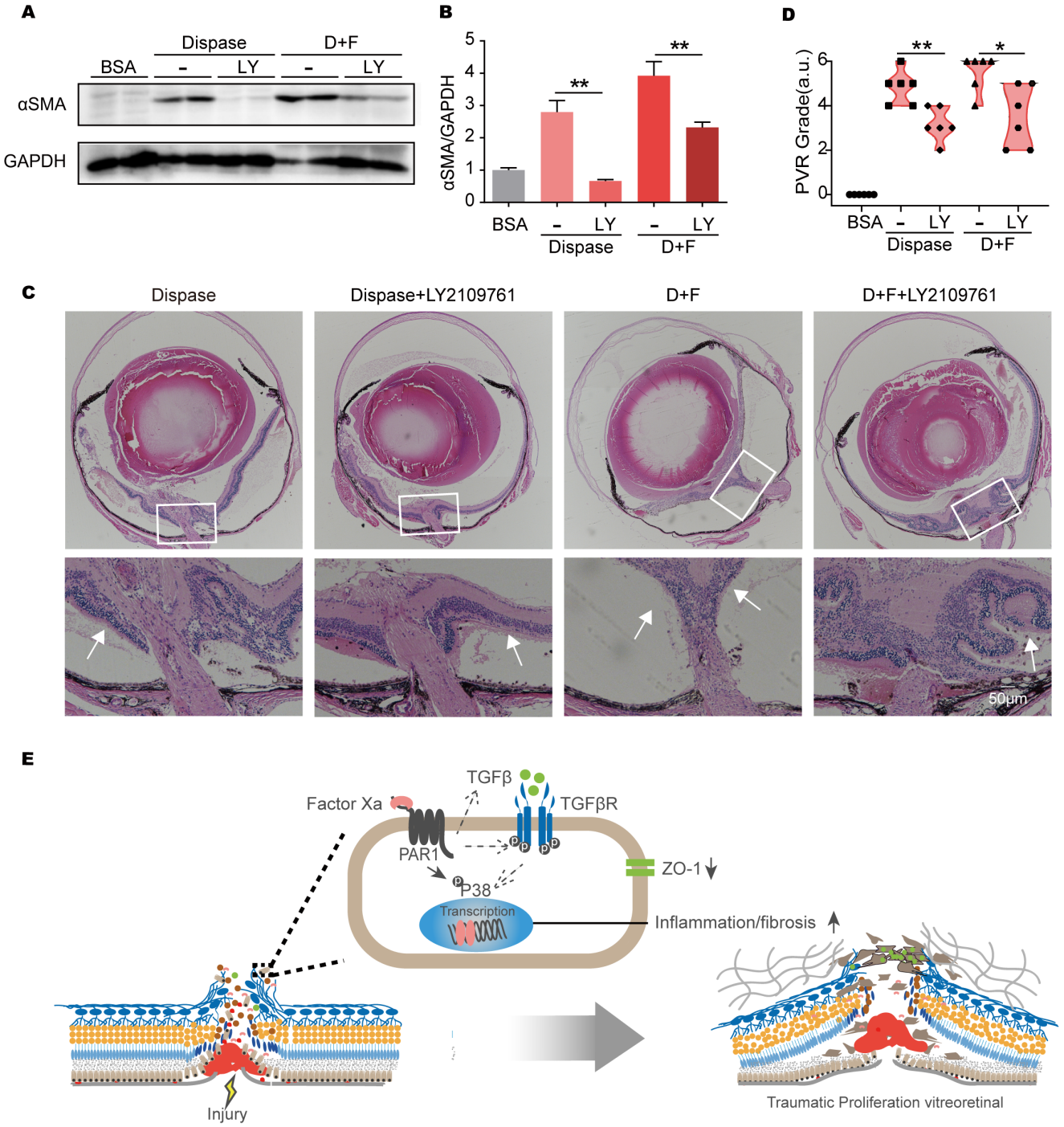

Figure 6. TGF-βR inhibitor blocks FXa-induced intraocular fibrosis. (**A**) Western blot analysis of α-SMA in retinas of mice from designated treatment groups. (**B**) Quantification of the Western blot of α-SMA shown in **A**. The α-SMA protein expression was normalized to GAPDH. n $\geq$ 4 mice per treatment group. (**C**). H&E stained retinal sections from dispase and dispase+FXa mice with or without pretreatment with TGF-βR inhibitor LY2109761. (**D**) Grading of PVR severity based on **C**. (**E**). After ocular trauma, vitreous levels of FXa were significantly increased which may make contact with RPE and promote RPE cells activation. FXa activated PAR1 in RPE cells and subsequent activation of P38 signaling to promote mesenchymal transition of PRE cells including disruption of epithelial tight junction and increase ECM protein expression. Meanwhile, TGF-β signaling also played a role in FXa-induced EMT in RPE cells. Values are means $\pm$ SEM, $^{*}P < 0.05$, $^{**}P < 0.01$, $^{***}P < 0.001$.

ment with Parmodulin 2 (PAR1 inhibitor) or SB202190 (p38 inhibitor) blocked FXa-induced upregulation of FN (Figs. 5J, 5K) and disruption of ZO-1 proteins (Figs. 5L, 5M). Collectively, these results demonstrated that FXa-induced EMT of RPE is mediated by PAR1 and P38 signaling.

TGF-β Signaling Also Play a Role in FXa-induced Fibrosis

The cross talk between FXa and TGF-β pathway have been reported in many studies, which FXa was shown to activate

TGF-β signaling through upregulation of TGF-β or via interaction with TGF-βRII.[28,29] Intriguingly, in our study, the mRNA of TGF-β was marked increased after FXa treatment (Fig. 5N). Besides, we found the concentrations of TGF-β were significantly elevated in the vitreous from patients with traumatic PVR compared with MH patients (Fig. 5O). In addition, treatment with TGF-βR inhibitor (LY2109761) effectively blocked FXa induced FN expression and ZO-1 disruption in ARPE-19 cells (Figs. 5J, 5M). In dispase or dispase +FXa treated mice, pretreatment with LY2109761 also markedly decreased the upregulation of α-SMA in these mice (Figs. 6A, 6B). Moreover, histological examination showed less severe PVR such as reduced retinal detachment and retinal folds in mice pretreated with LY2109761 versus those did not receive LY2109761 (Figs. 6C, 6D). Interestingly, we found FXa did not induce phosphorylation of SMAD2/3, the canonical downstream signaling of TGF-β, in ARPE-19 cells (Supplementary Fig. S4). Altogether, these results suggest that TGF-β signaling also played a role in FXa-induced fibrosis.

Discussion

Activation of coagulation factors occurs in mechanical ocular trauma, although *in vitro* studies showed coagulation factors such as FXa and thrombin stimulate a proinflammatory and profibrotic response in RPE cells,[11,16,25,30–33] whether they contribute to the pathogenesis of PVR *in vivo* is yet to be determined. Here, we report for the first time that FXa was significantly increased in the vitreous fluid and ERMs from patients with traumatic PVR. Besides, we demonstrated that FXa stimulated RPE EMT *in vitro*, and contributed to the retinal injury and fibrosis in a mouse model of PVR. Furthermore, the retinal injury and intraocular fibrosis in these mice can be significantly mitigated by pretreatment with oral FXa inhibitor. Mechanistic studies revealed that the profibrotic response of FXa was largely mediated by PAR1-P38 pathway, and TGF-β signaling also played a role in FXa-induced fibrosis.

The onset of PVR can occur between two weeks and six months after mechanical ocular trauma.[1] In our rabbit models, vitreous FXa after open globe injury was immediately increased and peaked at three days, then was gradually decreased thereafter, and vitreous FXa after closed globe injury was elevated and sustained for up to 28 days after the injury, suggesting that increased vitreous FXa after mechanical ocular trauma may participate in PVR pathogenesis. In addition, we found FXa levels were significantly elevated in the vitreous of traumatic PVR patients compared to patients with macular hole. Ricker et al.[12] reported high procoagulant activity in subretinal fluid collected from RRD patients who developed PVR within a two-month period as those without postsurgical PVR, although no significance was found between the two groups regarding the various parameters of the thrombogram. Nevertheless, high tissue factor (TF) levels in RRD patients were associated with poor visual prognosis (i.e., longer duration of macular detachment and worse preoperative visual acuity), suggesting a pathological role of intraocular procoagulant factors in vitreoretinal disorders. Besides, Bastiaans et al.[16] reported significantly increased thrombin activity in the vitreous of patients with established PVR compared to RRD patients without PVR development,[16] which is in accordance with our results. Overall, these studies support the role of intraocular procoagulant factors in the pathogenesis of vitreoretinal disorders.

To examine the actual role of FXa in PVR pathogenesis *in vivo*, we used a dispase-induced mouse PVR model.[18,23,34] PVR have been successfully induced in rabbit and mouse by employing surgical interventions or injection of cells, for example, fibroblasts or RPE cells, or dispase.[23,35] Injection of cells in the eye promoted PVR development very rapidly and are widely used, however, the involvement of large numbers of RPE cells in the eyes make it not suitable for current research. In comparison, dispase injection provide a relative safe and reproducible model of PVR without introduction of exogenous cells.[18] In our study, injection of dispase for 14 days effectively triggered PVR development including retinal detachment and fibrosis proliferation. Coadministration with FXa promoted a severer manifestation of PVR. Interestingly, we found FXa alone is not sufficient to promote PVR development. As BRB breakdown and RPE cells exposed to vitreous components are known predisposing conditions associated with PVR development,[1] the application of the proteolytic enzyme dispase may stimulate similar pathological conditions that exposing RPE cells to vitreous profibrotic factors such as FXa. Indeed, the expressions of α-SMA were significantly increased in dispase+FXa treated eyes compared to dispase or FXa treatment alone, supporting a profibrotic effect of FXa in mouse PVR model induced by dispase.

FXa inhibitor rivaroxaban and thrombin inhibitor dabigatran are clinically approved for bleeding disorders.[36,37] We tested the therapeutic effect of these anticoagulants in our PVR mouse models. We found a beneficial role of rivaroxaban and dabigatran in improving PVR as both inhibitors effectively reduced the expression of α-SMA and reduced the occurrence of retinal structural damage and retinal detachment in dispase- and FXa-treated mice, with rivaroxaban showed even better therapeutic effect than dabigatran. Future clinical studies are needed to validate our results, nevertheless, the effect of FXa and thrombin inhibitor might be worth testing in mechanical ocular trauma patients who are at high risk for developing PVR. Previous studies have shown that the biggest safety problem of oral anticoagulants is bleeding,[36] in our experiments, we also observed unexcepted intraocular bleeding in some mice after rivaroxaban or dabigatran treatment. Because intraocular hemorrhage was considered a risk factor for development of PVR, the occurrence of intraocular bleeding may offset the therapeutic benefits of oral anticoagulants. Therefore future studies are warranted to determine the best timing and dosage for application of oral anticoagulants after mechanical ocular trauma.

The cross-talk between FXa and TGF-β pathway have been reported in many studies; FXa was shown to activate latent TGF-β via PAR1-dependent mechanism in pulmonary fibrosis.[38] Others reported that PAR1 suppresses TGF-β signaling via competing with TGF-βRI for TGF-βRII binding, and PAR1 activation frees TGF-βRII for TGF-βRI binding, resulting in TGF-β signaling activation.[29] In our study, the mRNA expression of TGF-β was significantly upregulated on FXa stimulation, and FXa-induced RPE EMT can be mitigated by TGF-βR I/II inhibitor, suggesting a role for TGF-β signaling in FXa induced profibrotic effect. However, we did not observe phosphor activation of SMAD2/3 after FXa treatment in ARPE-19 cells (Supplementary Fig. S4) and that TGF-β2-induced FN expressions were not affected by PAR1 knockdown (Supplementary Fig. S5). Therefore how FXa

Investigative Ophthalmology & Visual Science

interacts with TGF-β pathway in RPE cells requires further research.

In conclusion, we found significantly increased FXa in the vitreous fluid of patients with traumatic PVR and in rabbit eyes after mechanical ocular trauma. We demonstrated that FXa promoted intraocular fibrosis via mechanisms involving RPE activation. Most importantly, application of FXa inhibitor significantly mitigated the retinal injury and intraocular fibrosis induced by dispase and FXa in mice. Overall, our data provide direct evidence of FXa inhibition in reducing PVR development in mice, suggesting that targeting FXa might become a potential therapeutic strategy for treating PVR.

Acknowledgments

Supported by National Natural Science Foundation of China (Grant Number 81830026, 81970828, 81800817), and Natural Science Foundation of Tianjin (Grant Number 18ZXDBSY00030).

Disclosure: **H. Han,** None; **X. Zhao,** None; **M. Liao,** None; **Y. Song,** None; **C. You,** None; **X. Dong,** None; **X. Yang,** None; **X. Wang,** None; **B. Huang,** None; **M. Du,** None; **H. Yan,** None

References

1. Morescalchi F, Duse S, Gambicorti E, Romano MR, Costagliola C, Semeraro F. Proliferative vitreoretinopathy after eye injuries: an overexpression of growth factors and cytokines leading to a retinal keloid. *Mediators Inflamm*. 2013;2013:269787.
2. Ozdek S, Hasanreisoglu M, Yuksel E. Chorioretinectomy for perforating eye injuries. *Eye*. 2013;27:722–727.
3. Schaub F, Enders P, Fauser S. Proliferative vitreoretinopathy: therapeutic strategies. *Klin Monatsbl Augenheilkd*. 2016;233:1016–1023.
4. Han L, Jia J, Fan Y, et al. The vitrectomy timing individualization system for ocular trauma (VTISOT). *Sci Rep*. 2019;9:12612.
5. Beuste T, Rebollo O, Parrat E, et al. Recurrences of retinal detachment after retinectomy: causes and outcomes. *Retina*. 2020;40:1315–1324.
6. Glaser BM, Cardin A, Biscoe B. Proliferative vitreoretinopathy. The mechanism of development of vitreoretinal traction. *Ophthalmology*. 1987;94:327–332.
7. Tamiya S, Liu L, Kaplan HJ. Epithelial-mesenchymal transition and proliferation of retinal pigment epithelial cells initiated upon loss of cell-cell contact. *Invest Ophthalmol Vis Sci*. 2010;51:2755–2763.
8. Tamiya S, Kaplan HJ. Role of epithelial-mesenchymal transition in proliferative vitreoretinopathy. *Exp Eye Res*. 2016;142:26–31.
9. Radeke MJ, Radeke CM, Shih YH, et al. Restoration of mesenchymal retinal pigmented epithelial cells by TGFbeta pathway inhibitors: implications for age-related macular degeneration. *Genome Medicine*. 2015;7:58.
10. Kita T, Hata Y, Arita R, et al. Role of TGF-beta in proliferative vitreoretinal diseases and ROCK as a therapeutic target. *PNAS*. 2008;105:17504–17509.
11. Bastiaans J, van Meurs JC, van Holten-Neelen C, et al. Factor Xa and thrombin stimulate proinflammatory and profibrotic mediator production by retinal pigment epithelial cells: a role in vitreoretinal disorders? *Graefes Arch Clin Exp Ophthalmol*. 2013;251:1723–1733.
12. Ricker LJ, Dieri RA, Beckers GJ, et al. High subretinal fluid procoagulant activity in rhegmatogenous retinal detachment. *Invest Ophthalmol Vis Sci*. 2010;51:5234–5239.
13. Ebrahimi S, Rezaei S, Seiri P, Ryzhikov M, Hashemy SI, Hassanian SM. Factor Xa signaling contributes to the pathogenesis of inflammatory diseases. *J Cell Physiol*. 2017;232:1966–1970.
14. Krupiczojc MA, Scotton CJ, Chambers RC. Coagulation signalling following tissue injury: focus on the role of factor Xa. *Int J Biochem Cell Biol*. 2008;40:1228–1237.
15. Borensztajn K, Peppelenbosch MP, Spek CA. Factor Xa: at the crossroads between coagulation and signaling in physiology and disease. *Trends Mol Med*. 2008;14:429–440.
16. Bastiaans J, van Meurs JC, Mulder VC, et al. The role of thrombin in proliferative vitreoretinopathy. *Invest Ophthalmol Vis Sci*. 2014;55:4659–4666.
17. Dhar A, Sadiq F, Anstee QM, Levene AP, Goldin RD, Thursz MR. Thrombin and factor Xa link the coagulation system with liver fibrosis. *BMC Gastroenterology*. 2018;18:60.
18. Soler MV, Gallo JE, Dodds RA, Suburo AM. A mouse model of proliferative vitreoretinopathy induced by dispase. *Exp Eye Res*. 2002;75:491–504.
19. Heffer A, Wang V, Sridhar J, et al. A mouse model of proliferative vitreoretinopathy induced by intravitreal injection of gas and RPE cells. *Transl Vis Sci Technol*. 2020;9:9.
20. Hirsch L, Nazari H, Sreekumar PG, et al. TGF-beta2 secretion from RPE decreases with polarization and becomes apically oriented. *Cytokine*. 2015;71:394–396.
21. Rhee DY, Zhao XQ, Francis RJ, Huang GY, Mably JD, Lo CW. Connexin 43 regulates epicardial cell polarity and migration in coronary vascular development. *Development*. 2009;136:3185–3193.
22. Hikita T, Mirzapourshafiyi F, Barbacena P, et al. PAR-3 controls endothelial planar polarity and vascular inflammation under laminar flow. *EMBO Rep*. 2018;19 (9):e45253.
23. Agrawal RN, He S, Spee C, Cui JZ, Ryan SJ, Hinton DR. *in vivo* models of proliferative vitreoretinopathy. *Nat Protoc*. 2007;2:67–77.
24. Hollborn M, Kohen L, Werschnik C, Tietz L, Wiedemann P, Bringmann A. Activated blood coagulation factor X (FXa) induces angiogenic growth factor expression in human retinal pigment epithelial cells. *Invest Ophthalmol Vis Sci*. 2012;53:5930–5939.
25. Bastiaans J, van Meurs JC, van Holten-Neelen C, et al. Thrombin induces epithelial-mesenchymal transition and collagen production by retinal pigment epithelial cells via autocrine PDGF-receptor signaling. *Invest Ophthalmol Vis Sci* 2013;54:8306–8314.
26. Schiff L, Boles N, Fernandes M, Nachmani B, Gentile R, Blenkinsop T. P38 inhibition reverses TGFβ1 and TNFα-induced contraction in a model of proliferative vitreoretinopathy. *Commun Biology*. 2019;2:162.
27. Saika S, Yamanaka O, Ikeda K, et al. Inhibition of p38MAP kinase suppresses fibrotic reaction of retinal pigment epithelial cells. *Lab Invest*. 2005;85:838–850.
28. Lin C, Rezaee F, Waasdorp M, et al. Protease activated receptor-1 regulates macrophage-mediated cellular senescence: a risk for idiopathic pulmonary fibrosis. *Oncotarget*. 2015;6:35304–35314.
29. Gong H, An S, Sassmann A, et al. PAR1 scaffolds TGFbetaRII to downregulate TGF-beta signaling and activate ESC differentiation to endothelial cells. *Stem Cell Rep*. 2016;7:1050–1058.
30. Hollborn M, Kohen L, Werschnik C, Tietz L, Wiedemann P, Bringmann A. Activated blood coagulation factor X (FXa) induces angiogenic growth factor expression in human retinal pigment epithelial cells. *Invest Ophthalmol Vis Sci*. 2012;53:5930–5939.

31. Yoshida A, Elner S, Bian Z, Kunkel S, Lukacs N, Elner V. Thrombin regulates chemokine induction during human retinal pigment epithelial cell/monocyte interaction. *Am J Pathol*. 2001;159:1171–1180.
32. Bian Z, Elner S, Elner V. Thrombin-induced VEGF expression in human retinal pigment epithelial cells. *Invest Ophthalmol Vis Sci*. 2007;48:2738–2746.
33. Hollborn M, Petto C, Steffen A, et al. Effects of thrombin on RPE cells are mediated by transactivation of growth factor receptors. *Invest Ophthalmol Vis Sci*. 2009;50:4452–4459.
34. Márkus B, Pató Z, Sarang Z, et al. The proteomic profile of a mouse model of proliferative vitreoretinopathy. *FEBS Open Bio*. 2017;7:1166–1177.
35. Hirose F, Kiryu J, Tabata Y, et al. Experimental proliferative vitreoretinopathy in rabbits by delivery of bioactive proteins with gelatin microspheres. *Eur J Pharm Biopharm*. 2018;129:267–272.
36. Gulseth M, Michaud J, Nutescu E. Rivaroxaban: an oral direct inhibitor of factor Xa. *Am J Health-System Pharm*. 2008;65:1520–1529.
37. Comin J, Kallmes DF. Dabigatran (Pradaxa). *AJNR Am J Neuroradiol*. 2012;33:426–428.
38. Scotton CJ, Krupiczojc MA, Konigshoff M, et al. Increased local expression of coagulation factor X contributes to the fibrotic response in human and murine lung injury. *J Clin Invest*. 2009;119:2550–2563.

Investigative Ophthalmology & Visual Science